Liquid–Liquid Phase Separation in Polysulfone/Solvent/Water Systems

JE YOUNG KIM,[1] HWAN KWANG LEE,[2] KI JUN BAIK,[3] SUNG CHUL KIM[1]

[1] Department of Chemical Engineering, Korea Advanced Institute of Science and Technology, 373-1, Kusong-Dong, Yusung-Gu, Taejon 305-701, South Korea

[2] Department of Industrial Chemistry, Chungnam Sanup University, #29, Namjang-Ri, Hongsung-Eub, Hongsung-Gun, Chungnam 350-800, South Korea

[3] Polymer Research Department, Daelim Industrial Co. Ltd., Yusung P.O. Box 116, Taejon 305-345, South Korea

Received 27 August 1996; accepted 16 January 1997

ABSTRACT: The cloud point curves for polysulfone (PSf)/solvent/water systems were determined by a titration method. A small amount of water was needed to induce liquid–liquid demixing and the temperature effect was small. From numerical calculations, it was found that the binary interaction parameters for the PSf/solvent/water system enlarges the homogeneous region in the phase diagram with a smaller nonsolvent–polymer interaction parameter χ_{13}, a greater nonsolvent–solvent interaction parameter χ_{12}, and a smaller solvent–polymer interaction parameter χ_{23} and the effect of polymer molecular weight was negligible except in the range of low molecular weight. The phase diagrams, calculated with constant χ_{12} that was chosen from the concentration-dependent interaction parameter g_{12} value of the concentration range, were similar to the results obtained with g_{12}. The slope of the tie lines indicated that demixing of the ternary system occurred at relatively similar nonsolvent concentration in both phases. A value of 2.7 for the water–PSf interaction parameter was obtained by fitting the experimental cloud point curve with the calculated binodal lines. © 1997 John Wiley & Sons, Inc. J Appl Polym Sci **65:** 2643–2653, 1997

INTRODUCTION

Polysulfone (PSf) is widely used as a membrane material since it has excellent chemical resistance, mechanical strength, thermal stability, and transport properties.[1] The preparation of polymeric membranes usually involves the phase-inversion process, in which a homogeneous polymer solution undergoes phase separation into a polymer-rich phase and a polymer-lean phase by the exchange of solvent with nonsolvent in a coagulation bath. Phase separation would continue to form the membrane structure until the polymer-rich phase is solidified.[2] Generally, solidification during phase separation may occur by gelation[3] and/or crystallization of the polymer,[3–5] but the PSf systems are not complicated by crystallization.[6,7]

While the final morphology obtained during phase inversion depends upon the kinetics as well as the thermodynamics of the phase separation, the equilibrium phase diagram is still a good tool for controlling the morphology and interpreting the membrane structure. Knowledge of phase equilibria (binodals, spinodals, and critical compositions) enables one to change the conditions for the preparation of membranes such as the temperatures and the compositions of the casting solution and of the coagulation bath to obtain an optimum structure.[2]

Correspondence to: S. C. Kim.
Contract grant sponsor: Daelim Industrial Co., Ltd.

Journal of Applied Polymer Science, Vol. 65, 2643–2653 (1997)
 CCC 0021-8995/97/132643-11

There are a few reports presenting the experimental phase diagrams in ternary mixtures of PSf/solvent/water.[6–8] The solvent systems studied were dimethylacetamide (DMAc), *N*-methyl-2-pyrrolidone (NMP), dimethylformamide (DMF), tetramethylurea (TMU), and *N,N*-dimethylpropyleneurea (DMPU). An interesting feature observed in the phase equilibria was that the system required a small amount of water to achieve liquid–liquid demixing, 3 wt % water for PSf/DMF/water, and 5–10 wt % water in other systems.[7] This is attributed to hydrophobic characteristics of PSf as indicated in the literature.[9,10] Alterna and Smolders showed by numerical calculation that the demixing behavior of PSf/solvent/nonsolvent systems is significantly influenced by the nonsolvent–polymer interaction parameter.[10]

In this work, we were concerned with a thermodynamic analysis of PSf/solvent/water systems. We used NMP and tetrahydrofuran (THF) as a solvent. Our objectives were to evaluate a value of the water–PSf interaction parameter by comparing the experimental cloud point curve with the calculated binodal curves based on the thermodynamics of polymer solutions and to provide a useful thermodynamic foundation to investigate phase-separation dynamics and the mechanism involved in membrane formation.

THERMODYNAMICS OF TERNARY SYSTEMS OF NONSOLVENT/SOLVENT/POLYMER

In this article, the Flory–Huggins lattice treatment[11,12] is used to describe the thermodynamics of the ternary system. The Flory–Huggins expression is extended with a concentration-dependent interaction parameter. The Gibbs free energy of mixing ΔG_M in ternary solutions is given by

$$\Delta G_M/RT = n_1 \ln \phi_1 + n_2 \ln \phi_2 + n_3 \ln \phi_3 + g_{12}(u_2) n_1 \phi_2 + \chi_{13} n_1 \phi_3 + \chi_{23} n_2 \phi_3 \quad (1)$$

where n_i are moles; ϕ_i, the volume fraction of component i; R, the gas constant; and T, the absolute temperature. The subscripts refer to nonsolvent (1), solvent (2), and polymer (3). χ_{13} is the nonsolvent–polymer interaction parameter, and χ_{23}, the solvent–polymer interaction parameter. g_{12} is the nonsolvent–solvent interaction parameter that is assumed to be a function of u_2 with $u_2 = \phi_2/(\phi_1 + \phi_2)$.[13] Since there are no data available for concentration-dependent interaction parameters g_{13} and g_{23}, the constant interaction parameters χ_{13} and χ_{23} are adopted instead. The effects of the polydispersity of polymer molecules are not taken into account in this calculation.

Binodal Curve

The calculation for equilibrium between two liquid phases I and II can be written as

$$\Delta\mu_i^{\mathrm{I}} = \Delta\mu_i^{\mathrm{II}} \; (i = 1, 2, 3) \quad (2)$$

where $\Delta\mu_i$ is the chemical potential of component i. Superscripts I and II refer to polymer-rich and polymer-lean phases, respectively. Also, the material balance requires

$$\sum \phi_i^{\mathrm{I}} = \sum \phi_i^{\mathrm{II}} = 1 \quad (3)$$

When the proper derivatives of the Gibbs free energy of mixing are taken, the chemical potential of component i, $\Delta\mu_i$, may be written as

$$\Delta\mu_1/RT = \ln \phi_1 + 1 - \phi_1 - \phi_2(v_1/v_2) - \phi_3(v_1/v_3) + (g_{12}\phi_2 + \chi_{13}\phi_3) \times (\phi_2 + \phi_3) - \chi_{23}\phi_2\phi_3(v_1/v_2) - u_2(1 - u_2)\phi_2(dg_{12}/du_2) \quad (4)$$

$$\Delta\mu_2/RT = \ln \phi_2 + 1 - \phi_2 - \phi_1(v_2/v_1) - \phi_3(v_2/v_3) + (g_{12}\phi_1(v_2/v_1) + \chi_{23}\phi_3) \times (\phi_1 + \phi_3) - \chi_{13}\phi_1\phi_3(v_2/v_1) + u_2(1 - u_2)\phi_1(v_2/v_1)(dg_{12}/du_2) \quad (5)$$

$$\Delta\mu_3/RT = \ln \phi_3 + 1 - \phi_3 - \phi_1(v_3/v_1) - \phi_2(v_3/v_2) + (\chi_{13}\phi_1(v_3/v_1) + \chi_{23}\phi_2(v_3/v_2)) \times (\phi_1 + \phi_2) - g_{12}\phi_1\phi_2(v_3/v_1) \quad (6)$$

where v_i is the molar volume of component i.

Given a set of interaction parameter and temperature, five coupled nonlinear equations [eqs. (2) and (3)] can be solved for the individual tie lines of coexisting phases with selection of one of the compositions as an independent variable. We selected ϕ_3^{II} (volume fraction of the polymer in the polymer-lean phase) as the independent variable. The Newton–Raphson method based on a least-square procedure was employed to solve the simultaneous equations.[10,14] To avoid a trivial solution ($\phi_i^{\mathrm{I}} = \phi_i^{\mathrm{II}}$), first, the initial guess values close

to the polymer–nonsolvent line were evaluated assuming that the polymer content in the polymer-lean phase is zero.[14]

Spinodal Curve and Critical Point

The spinodal that is the borderline between the unstable and metastable regions can be evaluated from the Tompa equation[12]:

$$G_{22}G_{33} = (G_{23})^2 \quad (7)$$

where $G_{ij} = [(\partial^2\overline{\Delta G_M})/(\partial\phi_i\,\partial\phi_j)]v_{\text{ref}}/RT$ and $\overline{\Delta G_M}$ is the Gibbs free energy of mixing on a unit-volume basis and v_{ref} is the molar volume of the reference component. From the relationship for ΔG_M, one has

$$G_{22} = 1/\phi_1 + (1/\phi_2)(v_1/v_2) - 2g_{12} + 2(1 - 2u_2) \times (dg_{12}/du_2) + u_2(1 - u_2)(d^2g_{12}/du_2^2) \quad (8)$$

$$G_{23} = 1/\phi_1 - (g_{12} + \chi_{13}) + \chi_{23}(v_1/v_2) + u_2(1 - 3u_2)(dg_{12}/du_2) + u_2^2(1 - u_2)(d^2g_{12}/du_2^2) \quad (9)$$

$$G_{33} = 1/\phi_1 + (1/\phi_3)(v_1/v_3) - 2\chi_{13} - 2u_2^3(dg_{12}/du_2) + u_2^3(1 - u_2)(d^2g_{12}/du_2^2) \quad (10)$$

To calculate the spinodal composition, one of the variables is chosen as the independent variable with the requirement of the material balance $\Sigma\,\phi_i = 1$ and the resulting single nonlinear equation can be solved numerically. The critical point for a ternary system can be calculated using the following expression,[12] with a spinodal condition:

$$G_{222}G_{33}^2 - 3G_{223}G_{23}G_{33} + 3G_{233}G_{23}^2 - G_{22}G_{23}G_{333} = 0 \quad (11)$$

Binary Interaction Parameters in PSf/Solvent/Water Systems

To calculate the phase diagram numerically, a set of three interaction parameter values should be known at a given temperature. The reported results relevant to our work is presented briefly.

The concentration-dependent interaction parameters g_{12} for water/NMP and water/THF systems are available from the literature sources.[15,16] The g_{12} functions are generally evaluated from the vapor–liquid equilibrium data of the binary mixture.[10,17] Figure 1 shows the binary interaction parameters for the pairs of water–NMP and water–THF systems at 25°C. The smaller value of g_{12} in water–NMP than in water–THF suggests that a stronger polar interaction exists in the water–NMP mixture. The difference in the strength of the interaction in each pair is more pronounced in the region of low water concentration.

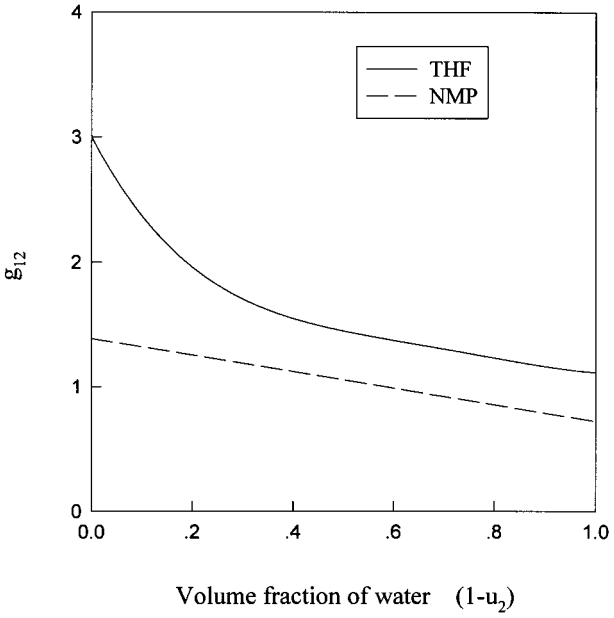

Figure 1 Concentration-dependent interaction parameters for the water–solvent system at 25°C.[15,16]

There are limited data on the solvent–polymer interaction parameter χ_{23}. Allen et al. determined the interaction parameter of the THF–PSf by viscometry and found it to be 0.46 at 25°C.[18] No data are available for the NMP–PSf pair. However, one may estimate the value of χ_{23} in NMP–PSf by investigating carefully the published results. The solubility of polyethersulfone (PES) is usually better than that of PSf in the same solvent as indicated by Swinyard and Barrie[7] and Lau et al.[8] Zeman and Tkacik showed by a light-scattering experiment that the χ_{23} value of the NMP–PES pair is in the range of 0.36–0.55 in the concentration range of 5–30 wt % PES.[15] Thus, the χ_{23} of NMP–PSf is expected to be slightly greater than that of NMP–PES. This speculation is supported by the fact that the χ_{23} of DMF–PES is 0.45 and that of DMF–PSf is 0.48 at 25°C.[18,19]

The nonsolvent–polymer interaction parameter χ_{13} may be determined from an equilibrium swelling experiment based on the Flory–Rehner

theory.[11] A published value in the water–PSf system is 3.7 at 25°C.[10] The measurement should be carried out in extremely high concentration of the polymer due to the hydrophobic character of PSf. The equilibrium water-sorption data at 20°C for PSf and PES are given as 0.85 and 2.1 wt %, respectively.[20] When considering the phase behavior of PSf/solvent/water, one would be interested in the region of a low concentration of the polymer. It was found that the χ_{13} value of the water–PES system is 2.66 by the water-sorption technique[21] but 1.6 in the concentration range of 5–25 wt % PES by the light-scattering method.[15]

EXPERIMENTAL

Materials

Polysulfone was Udel P-3500 purchased from Amoco Performance Products. The polymer had an $\overline{M_n}$ of 33,500 and an $\overline{M_w}$ of 50,800 obtained by size-exclusion chromatography. The solvents were *N*-methyl-2-pyrrolidinone (NMP) and tetrahydrofuran (THF) purchased from Aldrich Chemical Co. Both were HPLC grade and used without further purification. Distilled water was used as a nonsolvent.

Cloud Point Measurement

The cloud point curves were determined by a titration method at various temperatures of 15, 30, 45, and 60°C. Thermostated flasks with a rubber septum stopper were filled with 100 g of the polymer solution. The distilled water was added into the binary solution by a syringe through a septum, while thorough mixing was applied using a mechanical stirrer. Composition at the cloud point was determined by measuring the amount of water added when a visual turbidity was achieved.

Evaluation of the Water–Polymer Interaction Parameter χ_{13}

From the Flory–Rehner theory, χ_{13} is expressed as a simple equation[11]:

$$\chi_{13} = -[\ln(1 - \nu_p) + \nu_p]/\nu_p^2 \qquad (12)$$

where ν_p is the volume fraction of polymer and can be obtained by the swelling experiment. Dried strips of homogeneous PSf films (about 0.3–0.4 g with a thickness of 50–70 μm) were immersed in Petri dishes containing distilled water at 23°C. After 24 h, the strips were removed, pressed between tissue paper, and weighed in a closed flask. This procedure was continued until no further weight increase was observed.[22]

Table I Interaction Parameters for Solvent–PSf

Solvent	Measured Value[a]	Literature Value[b]	Reference
THF	0.39	0.46	18
NMP	0.24	—	—
Water	4.0	3.7	10

[a] Measured at 23°C.
[b] Measured at 25°C.

Evaluation of Solvent–Polymer Interaction Parameters χ_{23}

Solution viscosities of polysulfone in THF and NMP at 23°C were measured with a Ubbelohde viscometer. The intrinsic viscosity was determined by the usual extrapolation to zero concentration and the solvent–polymer interaction parameter was obtained by Kok's method.[23]

RESULTS AND DISCUSSION

First, we present the results on the interaction parameters. The solvent–PSf interaction parameter χ_{23} is determined by the measurement of the intrinsic viscosity which was proposed by Kok and Rudin[23] and the water–PSf interaction parameter χ_{13} is measured by a water-sorption method.[22] The χ_{23} value of the THF–PSf system at 23°C was 0.39, similar to the reported value 0.46 at 25°C.[18] The χ_{23} value of the NMP–PSf system at 23°C was 0.24, as expected lower than that of THF–PSf. For the water–PSf system, we obtained the χ_{13} value of 4.0 at 23°C with some scatter of data compared to a published value of 3.7 at 25°C. The measured values are summarized in Table I, together with the literature data.

Figure 2 gives the experimental cloud point curves of the systems of PSf/THF/water [Fig. 2(a)] and PSf/NMP/water [Fig. 2(b)] at 15 and 60°C, which show the miscible region of polymer and solvent with water. We do not show the cloud point curves for 30 and 45°C in Figure 2 for the sake of clarity and do show the effect of temperature in terms of precipitation value of water in

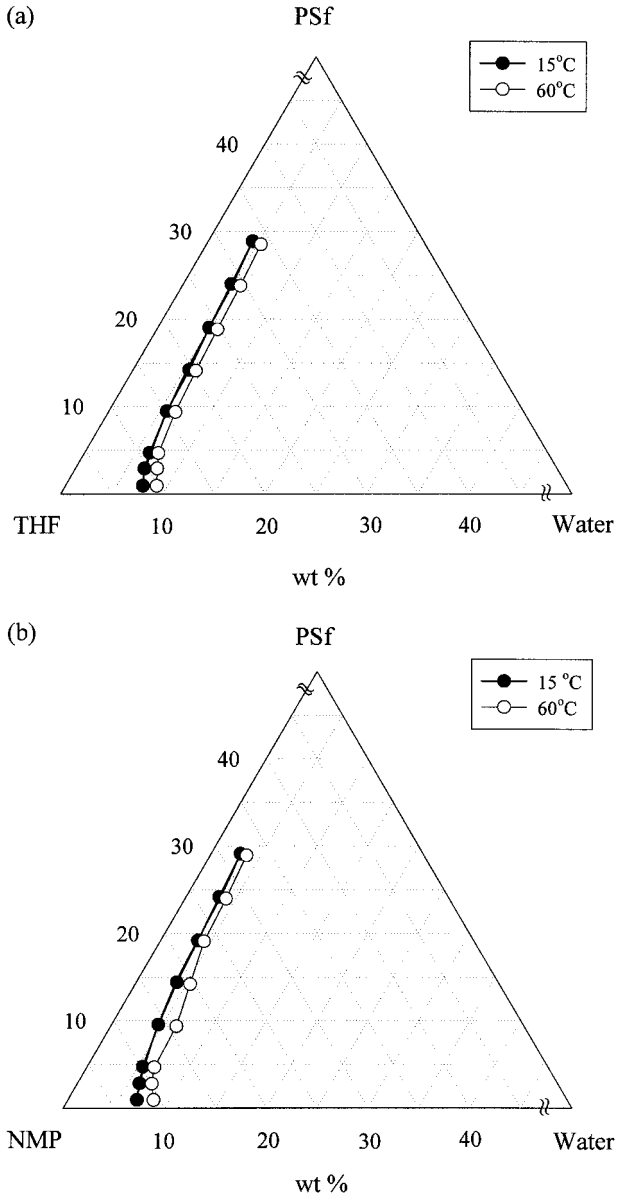

Figure 2 Cloud point curves of (a) PSf/THF/water and (b) PSf/NMP/water at 15 and 60°C.

PSf solutions (grams of water per 100 g of polymer solution to obtain phase separation) in Figure 3.

An obvious feature in Figure 2 is that a small amount of water is needed to induce liquid–liquid demixing and the region of the homogeneous phase is enlarged slightly with increasing temperature. The effect of temperature on the cloud point curve may indicate that the temperature dependence of interaction parameters is relatively small. Another observation is that the region of the homogeneous phase is larger in the PSf/THF/water system than in the PSf/NMP/water system at the same temperature. Thus, 5.8 g of water is required for 100 g of 15 wt % PSf solution with THF and 4.2 g of water for the same concentration of polymer with NMP at 15°C as shown in Figure 3. In this case, we have two conflicting effects on the phase diagram. As will be discussed later, one is the solvent–polymer interaction parameter (χ_{23}) effect which produces apparently a more homogeneous region for the PSf/NMP/water system

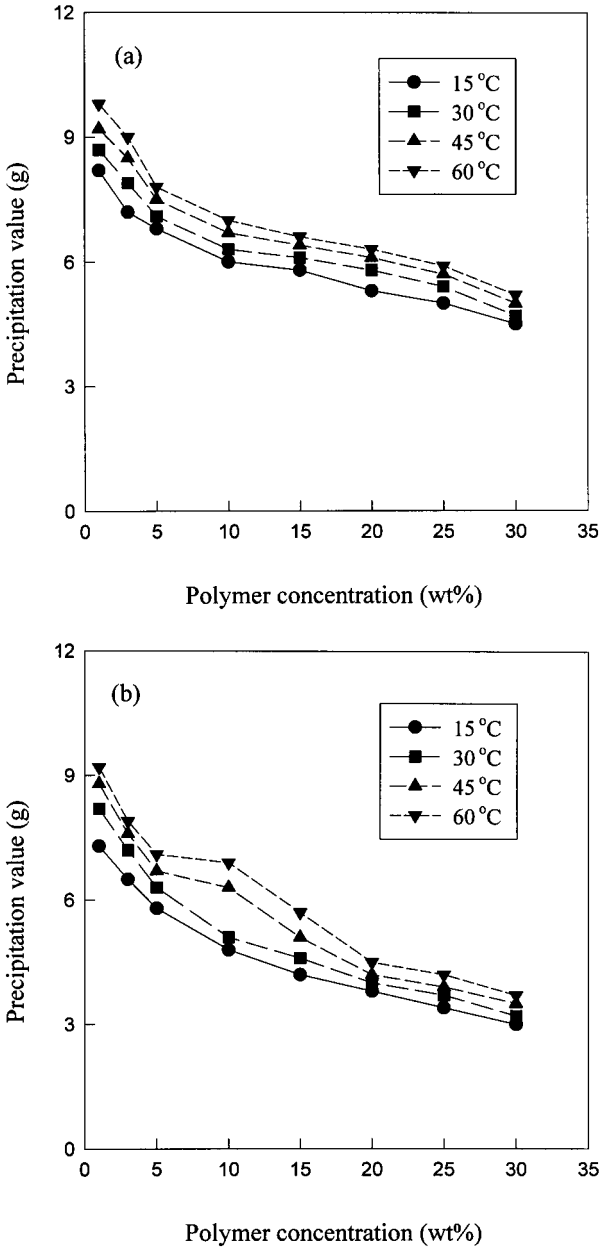

Figure 3 Precipitation values of water as a function of polymer concentration (grams of water per 100 g of polymer solution) for solutions of (a) PSf–THF and (b) PSf–NMP at various temperatures.

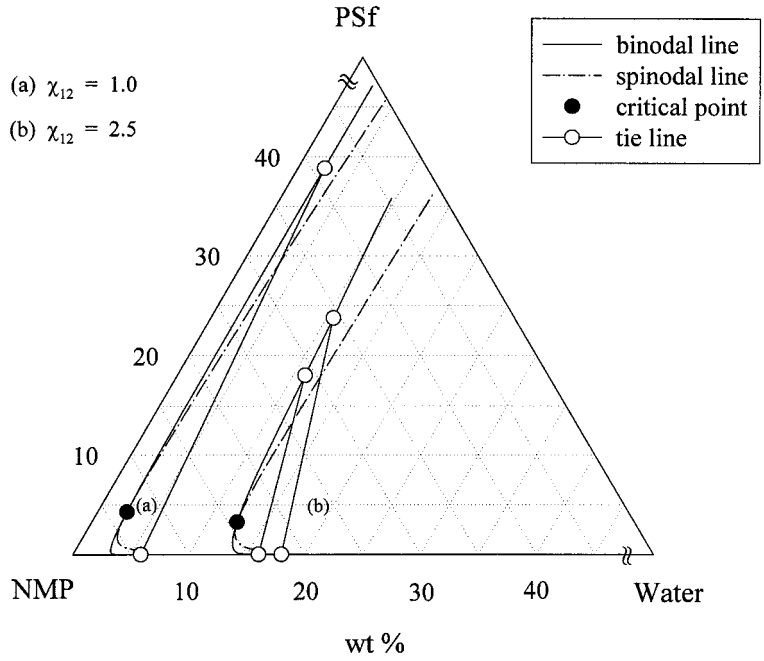

Figure 4 Calculated phase diagrams showing binodal, spinodal, critical compositions, and tie lines for (a) $\chi_{12} = 1.0$ and (b) $\chi_{12} = 2.5$ with $\chi_{23} = 0.24$ and $\chi_{13} = 3.0$.

(note Table I) and the other is the water–solvent interaction parameter (χ_{12}) effect which increases the homogeneous area for the PSf/THF/water system due to a higher value of χ_{12} (Fig. 1). The observed phase behavior suggests that the effect of χ_{12} is more pronounced than that of χ_{23} in PSf/solvent/water systems. It seems that there exists a specific interaction between NMP and water due to the polar nature of both components, which gives rise to producing a polar complex of one

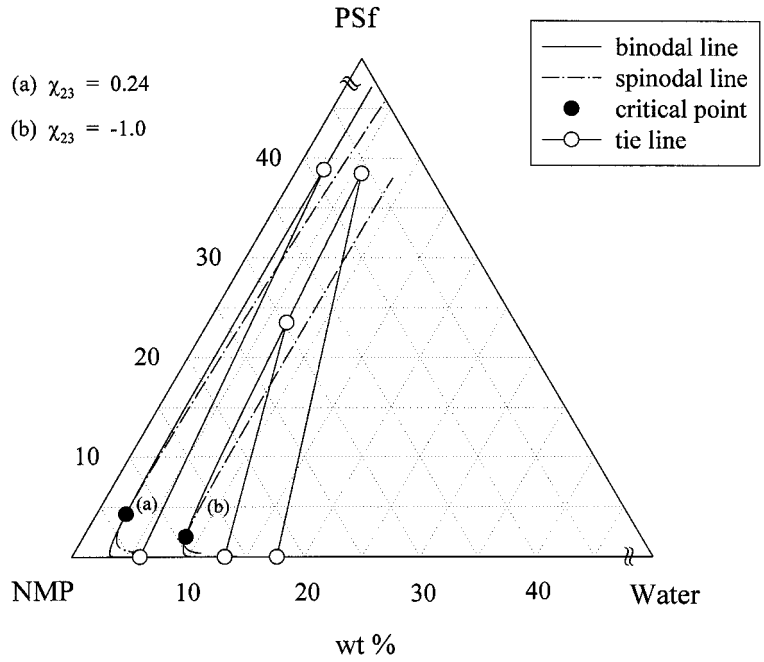

Figure 5 Calculated phase diagrams showing binodal, spinodal, critical compositions, and tie lines for (a) $\chi_{23} = 0.24$ and (b) $\chi_{23} = -1.0$ with $\chi_{12} = 1.0$ and $\chi_{13} = 3.0$.

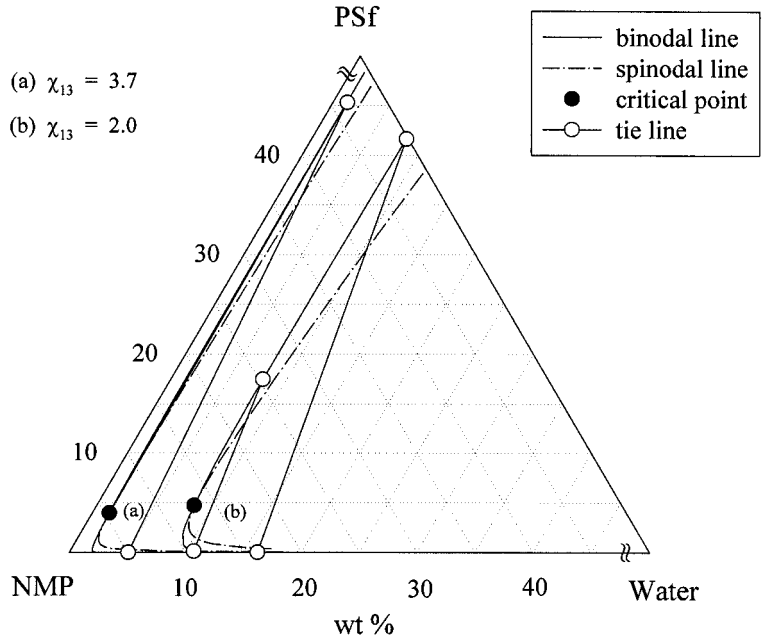

Figure 6 Calculated phase diagrams showing binodal, spinodal, critical compositions, and tie lines for (a) $\chi_{13} = 3.7$ and (b) $\chi_{13} = 2.0$ with $\chi_{12} = 1.0$ and $\chi_{23} = 0.24$.

NMP molecule and two water molecules,[15] resulting in a low χ_{12} value.

Now, we discuss the calculated phase diagrams including binodal lines, spinodal lines, critical compositions, and tie lines. To elucidate the effect of interaction parameters, first we use constant interaction parameters (χ_{12}, χ_{23}, χ_{13}). Considering the thermodynamics of the polymer solution

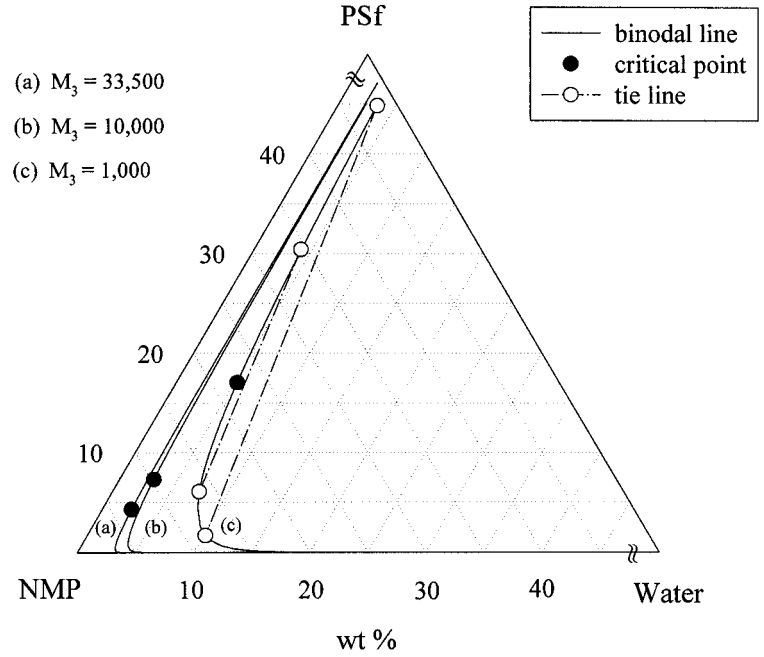

Figure 7 Calculated phase diagrams showing binodal, critical compositions, and tie lines for molar mass of polymer (a) $M_3 = 33{,}500$, (b) $M_3 = 10{,}000$, and (c) $M_3 = 1000$ with $\chi_{12} = 1.0$, $\chi_{23} = 0.24$, and $\chi_{13} = 3.0$.

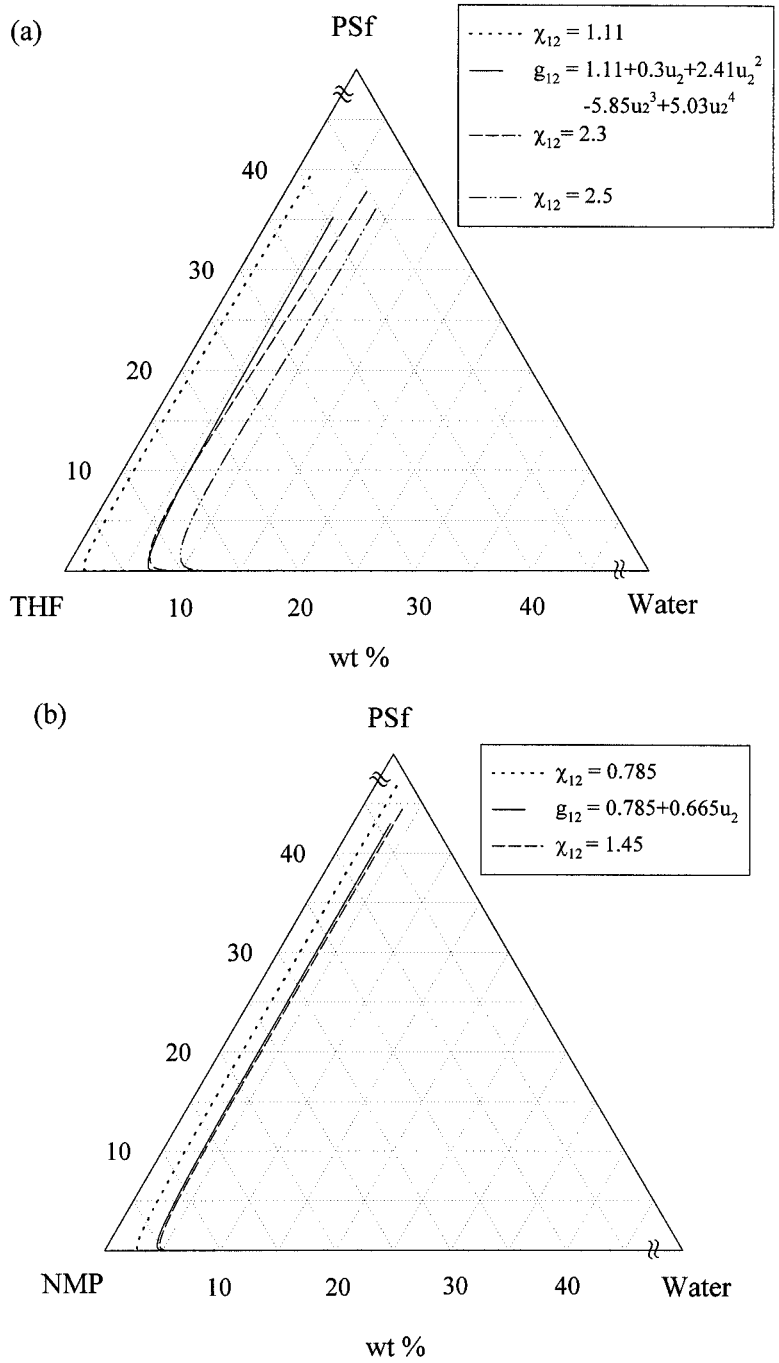

Figure 8 Comparison of binodal lines between the cases of constant χ_{12} and concentration-dependent g_{12} parameters in PSf/THF/water with (a) $\chi_{23} = 0.46$ and $\chi_{13} = 3.0$ in PSf/NMP/water with (b) $\chi_{23} = 0.24$ and $\chi_{13} = 3.0$.

described earlier, one can obtain a phase diagram in terms of the volume fraction of each component given a set of binary interaction parameters and molar volume ratios of v_1/v_2 and v_1/v_3. In the PSf/NMP/water system, a v_1/v_2 value of 0.188 for water–NMP was used for the calculation. Following Flory's recommendation,[11] the number-average molar mass of PSf (M_3 = 33,500) was used to obtain the molar volume of the polymer in all cases except in Figure 7. The calculated composition was converted into wt % to give a ternary phase diagram.

We arbitrarily chose sets of values relevant to the PSf/solvent/water system to investigate the effect of interaction parameters and polymer molecular weight. Figure 4 shows two sets of phase diagrams with different χ_{12} values of 1.0 and 2.5 while keeping the other parameters constant (χ_{23} = 0.24 and χ_{13} = 3.0). With an increasing χ_{12} parameter, the miscible region increases. It is understood that low miscibility between nonsolvent and solvent influences the solubility between polymer and solvent, resulting in a larger miscible region. Another important feature is a slight change of the slope of the tie line with increasing χ_{12} values. As the slope of the tie line increases to infinity, the polymer concentration of the polymer-rich phase may decrease, resulting in the delay of solidification. The metastable region which is located between binodal and spinodal lines increases slightly with a larger χ_{12} value in Figure 4.

The influence of the solvent–polymer interaction parameter χ_{23} is illustrated in Figure 5, while keeping χ_{12} and χ_{23} constant (χ_{12} = 1.0 and χ_{13} = 3.0). As expected, a lower value of χ_{23} increases the miscible region. We compared the χ_{23} of 0.24 with that of −1.0, which may be an impossible situation for this polymer solution. The χ_{23} value is usually in the range of 0.2–0.6, which definitely gives rise to little difference in the phase diagram. This is consistent with the phase behavior of PSf/THF/water and PSf/NMP/water systems. Thus, the effect of a small decrease of χ_{23} from 0.39 to 0.24 is overwhelmed by an increase of χ_{12}, as can be seen in Figure 2.

A lower value of the nonsolvent–polymer interaction parameter χ_{13} increases the miscible area as shown in Figure 6 (χ_{12} = 1.0 and χ_{23} = 0.24). We compared the cases of the χ_{13} of 3.7 and that of 2.0 which changed the phase boundary significantly. Practically, this range of χ_{13} is reasonable for relatively hydrophobic polymers. Hydrophilic polymers like cellulose acetate with the χ_{13} of 1.0 exhibit a much wider miscible region in the phase diagram.[10] It is apparent in Figures 5 and 6 that the slope of tie lines is almost parallel to the polymer–solvent axis for the range of interaction parameters in the PSf/solvent/water system. This suggests that the demixing of the polymer solution occurs at relatively constant nonsolvent concentrations and that the two separated phases differ mainly in their concentration of polymer and solvent.

Figure 7 shows that the decrease of polymer molecular weight from 33,500 to 10,000 changes negligibly the location of the binodal but increases the critical concentration of polymer from 3.7 to 6.5 wt %. The location of the binodal line is largely

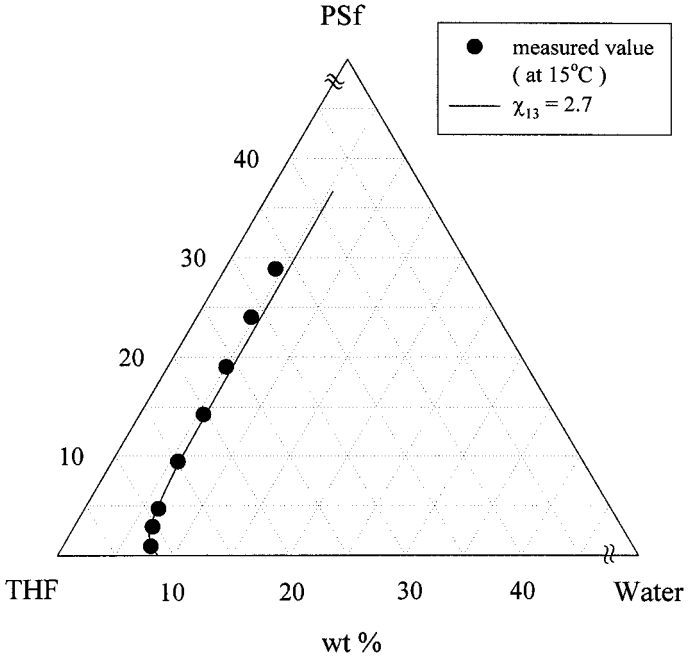

Figure 9 Comparison of experimental cloud point curve at 15°C and calculated binodal curve for the PSf/THF/water system with $g_{12} = 1.11 + 0.3u_2 + 2.41u_2^2 - 5.85u_2^3 + 5.03u_2^4$ and $\chi_{23} = 0.46$.

influenced by the polymer molecular weight only when the polymer molecular weight is extremely low. The critical composition determines which phase is nucleated for the nucleation and growth process on membrane formation. There are two possibilities, depending on the composition of the initial polymer solution with respect to the critical point: For a higher polymer concentration ϕ_3 than critical polymer concentration $\phi_{cr,3}$, the nuclei consist of the dilute phase, and in the other case, the nuclei consist of the polymer-rich phase. When phase separation starts with the critical composition ($\phi_3 = \phi_{cr,3}$), the structure formation is dominated by spinodal decomposition.[24] Since a typical membrane-forming solution contains higher than 10 wt % of polymer concentration, it is expected to undergo liquid–liquid phase separation with nucleation and growth of the dilute phase.

It would be interesting to compare the phase diagrams with the constant nonsolvent–solvent interaction parameter χ_{12} and with the concentration-dependent parameter g_{12}. Figure 8 indicates that when a constant χ_{12} value of 2.3 for water–THF and that of 1.4 for water–NMP are selected from the g_{12} values in the range of 3–10 vol % water, the calculated phase diagrams roughly match the phase diagrams obtained with the concentration-dependent g_{12}. Thus, an arbitrarily selected χ_{12} value such as 1.45 for water–THF[16] and 1.0 for water–NMP[25] may lead to an erroneous result.

Our calculation indicates clearly that the phase behavior of PSf/solvent/water is significantly influenced by the nonsolvent–polymer interaction parameter χ_{13}. We attempted to determine a proper value of χ_{13} in the PSf/solvent/water system since we had failed to fit the calculated binodal with our experimental cloud point curve with a reported value of 3.7.[10] We chose the concentration-dependent interaction parameter g_{12} and were able to fit the calculated binodal with the cloud point curve for PSf/THF/water with the χ_{13} of 2.7 as shown in Figure 9. In this case, we used the THF–PSf interaction parameter χ_{23} of 0.46 and the PSf molar mass of 33,500. Since the water–PSf interaction parameter from the water-sorption method is measured in a higher than 99 wt % polymer concentration, the proper χ_{13} value for the ternary polymer solution may be quite different. In fact, for the water–PES system, the χ_{13} was 2.66 by the water-sorption technique but 1.6 for the 5–25 wt % polymer concentration of the PES/NMP/water system by the light-scattering method.[15] Similarly, the χ_{13} value of 2.7 for the PSf/THF/water system seemed to be reasonable with a value of 3.7 by a water-sorption method.

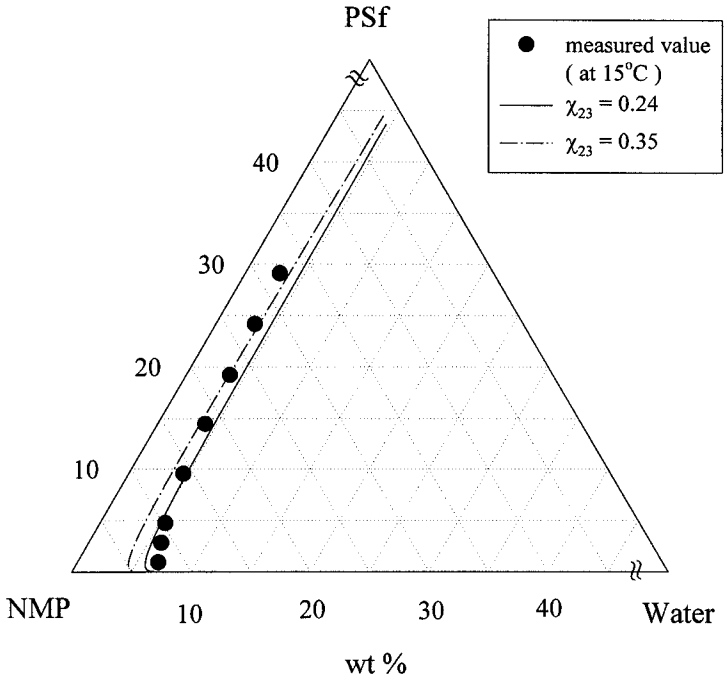

Figure 10 Comparison of experimental cloud point curve at 15°C and calculated binodal curve for the PSf/NMP/water system with $g_{12} = 0.785 + 0.665u_2$ and $\chi_{13} = 2.7$.

In the case of PSf/NMP/water, we also chose the concentration-dependent interaction parameter g_{12} with $\chi_{13} = 2.7$ determined from the analysis of the PSf/THF/water system. In contrast to the PSf/THF/water system, the shape of the cloud point curve deviated somewhat from the calculated binodal as can be seen in Figure 10. When a value of 0.35 was assigned to the χ_{23}, the curve matched the experimental results above 15 wt % polymer concentration but showed deviations for a low concentration of the polymer. A similar result on the cloud point curve of the PSf/NMP/water system was reported.[7,8] To explain the particular phase behavior of the PSf/NMP/water system, one has to introduce a concentration-dependent solvent–polymer interaction parameter g_{23}, which probably exhibits a lower g_{23} value in low concentrations of the polymer.

CONCLUSIONS

The cloud point curves for ternary systems of PSf/THF/water and PSf/NMP/water were determined by a titration method at 15, 30, 45, and 60°C. A small amount of water (3–10 wt % water) was needed to achieve liquid–liquid phase separation in both systems and the temperature effect was small.

From the numerical calculation, it was found that the binary interaction parameters for the PSf/solvent/water system enlarges the homogeneous region in the phase diagram with a smaller χ_{13}, a greater χ_{12}, and a smaller χ_{23} and the effect of the polymer molecular weight was negligible except in the range of low molecular weight. The phase diagrams, calculated with a constant interaction parameter χ_{12} that was chosen from the concentration-dependent interaction parameter g_{12} value of the concentration range, were similar to the results obtained with g_{12}. The slope of the tie lines indicated that demixing of the ternary system occurred at a relatively similar nonsolvent concentration in both phases. We obtained a value of 2.7 for the water–PSf interaction parameter by fitting the experimental cloud point curve with the calculated binodal lines. A concentration-dependent polymer–solvent interaction parameter was expected to fit better the cloud point curve for the PSf/NMP/water system.

The authors wish to acknowledge gratefully the financial support of Daelim Industrial Co., Ltd., for this work.

REFERENCES

1. E. Staude and L. Breitbach, *J. Appl. Polym. Sci.,* **43,** 559 (1991).
2. M. H. V. Mulder, *Basic Principles of Membrane Technology,* Elsevier, Amsterdam, 1991.
3. G. E. Gaides and A. J. McHugh, *Polymer,* **30,** 2118 (1989).
4. J. H. Aubert, *Macromolecules,* **21,** 3468 (1988).
5. H. C. Vadalia, H. K. Lee, A. S. Myerson, and K. Levon, *J. Membr. Sci.,* **89,** 37 (1994).
6. J. G. Wijmans, J. Kant, M. H. V. Mulder, and C. A. Smolders, *Polymer,* **26,** 1539 (1985).
7. B. T. Swinyard and J. A. Barrie, *Br. Polym. J.,* **20,** 317 (1988).
8. W. W. Y. Lau, M. D. Guiver, and T. Matsuura, *J. Membr. Sci.,* **59,** 219 (1991).
9. W. W. Y. Lau, M. D. Guiver, and T. Matsuura, *J. Appl. Polym. Sci.,* **42,** 3215 (1991).
10. F. W. Altena and C. A. Smolders, *Macromolecules,* **15,** 1491 (1982).
11. P. J. Flory, *Principles of Polymer Chemistry,* Cornell University Press, Ithaca, NY, 1953.
12. H. Tompa, *Polymer Solutions,* Butterworths, London, 1956.
13. J. Pouchly, A. Zivny, and K. Solc, *J. Polym. Sci. Part C,* **23,** 245 (1968).
14. L. Yilmaz and A. J. McHugh, *J. Appl. Polym. Sci.,* **31,** 997 (1986).
15. L. Zeman and G. Tkacik, *J. Membr. Sci.,* **36,** 119 (1988).
16. A. J. Reuvers, PhD Thesis, University of Twente, The Netherlands, 1987.
17. J. M. Prausnitz, R. N. Lichtenthaler, and E. Gomes de Azedo, *Molecular Thermodynamics of Fluid-Phase Equilibria,* 2nd ed., Prentice-Hall, Englewood Cliffs, NJ, 1986.
18. G. Allen, J. McAinsh, and C. Strazielle, *Eur. Polym. J.,* **5,** 319 (1969).
19. G. Allen and J. McAinsh, *Eur. Polym. J.,* **6,** 1635 (1970).
20. T. A. Tweddle, O. Kutowy, W. L. Thayer, and S. Sourirajan, *Ind. Eng. Chem. Prod. Res. Dev.,* **22,** 320 (1983).
21. V. B. Singh, J. A. Barrie, and D. J. Walsh, *J. Appl. Polym. Sci.,* **31,** 295 (1986).
22. M. H. V. Mulder and C. A. Smolders, *J. Membr. Sci.,* **17,** 289 (1984).
23. C. M. Kok and A. Rudin, *J. Appl. Polym. Sci.,* **27,** 353 (1982).
24. L. Broens, F. W. Altena, and C. A. Smolders, *Desalination,* **32,** 33 (1980).
25. R. M. Boom, T. van den Boomgaard, and C. A. Smolders, *Macromolecules,* **27,** 2034 (1994).